

# Interaction between the Conjugated Polyelectrolyte Poly{1,4-phenylene[9,9-bis(4-phenoxybutylsulfonate)]fluorene-2,7-diyl} Copolymer and the Lecithin Mimic 1-*O*-(L-Arginyl)-2,3-*O*-dilauroyl-*sn*-glycerol in Aqueous Solution

María J. Tapia,<sup>\*,†</sup> Hugh D. Burrows,<sup>\*,‡</sup> Matti Knaapila,<sup>§</sup> Andrew P. Monkman,<sup>§</sup> Antonio Arroyo,<sup>†</sup> Swapna Pradhan,<sup>||</sup> Ullrich Scherf,<sup>||</sup> Aurora Pinazo,<sup>⊥</sup> Lourdes Pérez,<sup>⊥</sup> and Carmen Morán<sup>⊥</sup>

*Departamento de Química, Universidad de Burgos, Plaza Misael Bañuelos s/n, 09001 Burgos, Spain, Departamento de Química, Universidade de Coimbra, 3004-535 Coimbra, Portugal, Department of Physics, University of Durham, South Road, Durham DH1 3LE, United Kingdom, Makromolekulare Chemie, Bergische Universität Wuppertal, D-42097 Wuppertal, Germany, and Institut d'Investigacions Químiques i Ambientals de Barcelona CSIC, Jordi Girona 18-26, 08034 Barcelona, Spain*

Received May 2, 2006. In Final Form: August 8, 2006

In this paper, the interaction between the water-soluble conjugated polyelectrolyte poly{1,4-phenylene[9,9-bis(4-phenoxybutylsulfonate)]fluorene-2,7-diyl} copolymer and the amino acid glyceride conjugate 1-*O*-(L-arginyl)-2,3-*O*-dilauroyl-*sn*-glycerol dichlorohydrate (a mimic for the phospholipid lecithin) has been studied in aqueous solution by electronic spectroscopy (absorption and fluorescence) and small-angle neutron scattering (SANS). A significant increase in the polymer fluorescence and blue shift in its emission are observed on association with the surfactant. This is suggested to be due to breakup of polymer aggregates. In addition, the spectroscopic and photophysical data suggest this is followed by the vesicle to ribbon transition characteristic of this surfactant, leading to incorporation of single chains of the polymer within mixed polymer–surfactant aggregates. Support for this comes from preliminary SANS measurements, from which evidence for polymer dissolution and formation of two-dimensional structures has been obtained.

## Introduction

Conjugated polyelectrolytes are proving to be attractive sensors for both chemical and biological applications.<sup>1–5</sup> Luminescence methods are particularly important for these systems and can combine high sensitivity with selectivity. Since the first reports by Whitten and co-workers of the enhancement of the fluorescence quantum yield of the anionic polymer poly(2,5-methoxypropyl-oxysulfonatephenylenevinylene) on complexing with the cationic dodecyltrimethylammonium bromide,<sup>1</sup> a number of other studies have reported the effect of surfactants on the photophysical behavior of these conjugated polyelectrolytes,<sup>6–10</sup> and this has led to the introduction of the concept of “surfactochromic” changes.<sup>6</sup>

Fluorene-based conjugated polymers and copolymers are of particular interest due to their unique combination of photo-

physical, spectroscopic, electronic, and materials properties, which make them versatile materials for optical and optoelectronic devices,<sup>11–12</sup> and they have found applications as light-emitting diodes,<sup>13–18</sup> photovoltaic cells,<sup>19</sup> lasers,<sup>20</sup> etc. Ionic derivatives of these fluorene copolymers have been shown to be particularly valuable as sensors for biological macromolecules,<sup>1</sup> including DNA<sup>2,3</sup> and proteins.<sup>4</sup>

In general, polyfluorenes form complicated self-assembled structures.<sup>21</sup> Hence, it is not surprising that polyfluorene-based

\* To whom correspondence should be addressed. (M.J.T.) E-mail: mjtapia@ubu.es. Fax: (+34) 947 28831. (H.D.B.) E-mail: burrows@ci.uc.pt. Fax: (+351) 239 827703.

<sup>†</sup> Universidad de Burgos.

<sup>‡</sup> Universidade de Coimbra.

<sup>§</sup> University of Durham.

<sup>||</sup> Bergische Universität Wuppertal.

<sup>⊥</sup> Institut d'Investigacions Químiques i Ambientals de Barcelona CSIC.

(1) Chen, L.; McBranch, D. W.; Wang, H.-L.; Helgeson, R.; Wudl, F.; Whitten, D. G. *Proc. Natl. Acad. Sci. U.S.A.* **1999**, *96*, 12287–12292.

(2) Gaylord, B. S.; Heeger, A. J.; Bazan, G. C. *J. Am. Chem. Soc.* **2003**, *125*, 896–900.

(3) Ho, H.; Boissinot, M.; Bergeron, M. G.; Corbeil, G.; Doré, K.; Boudreau, D.; Leclerc, M. *Angew. Chem., Int. Ed.* **2002**, *41*, 1548–1551.

(4) Fan, C.; Plaxco, K. W.; Heeger, A. J. *J. Am. Chem. Soc.* **2002**, *124*, 5642–5643.

(5) Tan, C.; Atas, E.; Müller, J. G.; Pinto, M. R.; Kleiman, V. D.; Schanze, K. S. *J. Am. Chem. Soc.* **2004**, *126*, 13685–13694.

(6) Lavigne, J. J.; Broughton, D. L.; Wilson, J. N.; Erdogan, B.; Bunz, U. H. F. *Macromolecules* **2003**, *36*, 7409–7412.

(7) Chen, L.; McBranch, D.; Wang, R.; Whitten, D. *Chem. Phys. Lett.* **2000**, *330*, 27–33.

(8) Burrows, H. D.; Lobo, V. M. M.; Pina, J.; Ramos, M. L.; Seixas de Melo, J.; Valente, A. J. M.; Tapia, M. J.; Pradhan, S.; Scherf, U. *Macromolecules* **2004**, *37*, 7425–7427.

(9) Tapia, M. J.; Burrows, H. D.; Valente, A. J. M.; Pradhan, S.; Scherf, U.; Lobo, V. M. M.; Pina, J.; Seixas de Melo, J. *J. Phys. Chem. B* **2005**, *109*, 19108–19115.

(10) Burrows, H. D.; Lobo, V. M. M.; Pina, J.; Ramos, M. L.; Seixas de Melo, J.; Valente, A. J. M.; Tapia, M. J.; Pradhan, S.; Scherf, U.; Hintschich, S. I.; Rothe, C.; Monkman, A. P. *Colloids Surf., A* **2005**, *270*–271, 61–66.

(11) Leclerc, M. *J. Polym. Sci., Part A: Polym. Chem.* **2001**, *39*, 2867–2873.

(12) Scherf, U.; List, E. J. W. *Adv. Mater.* **2002**, *14*, 477–487.

(13) Bliznyuk, V.; Ruhstaller, B.; Brock, P. J.; Scherf, U.; Carter S. A. *Adv. Mater.* **1999**, *11*, 1257–1261.

(14) Higgins, R. W. T.; Monkman, A. P.; Nothofer, G.-G.; Scherf, U. *Appl. Phys. Lett.* **2001**, *79*, 857–859.

(15) Millard, I. S. *Synth. Met.* **2000**, *111*–112, 119–123.

(16) Yang, X. H.; Jaiser, F.; Neher, D.; Lawson, P. V.; Brédas, J. L.; Zojer, E.; Güntner, R.; Freitas, P. S.; Forster, M.; Scherf, U. *Adv. Funct. Mater.* **2004**, *14*, 1097–1103.

(17) Plok, R.; Gamerith, S.; Gadermaier, C.; Plank, H.; Wenzl, F. P.; Patil, S.; Montenegro, R.; Kietzke, T.; Neher, D.; Scherf, U.; Landfester, K.; List, E. J. W. *Adv. Mater.* **2003**, *15*, 800–804.

(18) Pogantsch, A.; Wenzl, F. P.; List, E. J. W.; Leising, G.; Grimsdale, A. C.; Müllen, K. *Adv. Mater.* **2002**, *14*, 1061–1063.

(19) Akbayir, C.; Bulut, F.; Farrell, T.; Goldschmidt, A.; Güntner, R.; Kam, A. P.; Miclea, P.; Scherf, U.; Seekamp, J.; Solov'yev, V. G.; Sotomayor Torres, C. M. *Rev. Adv. Mater. Sci.* **2003**, *5*, 205–210.

(20) Heliotis, G.; Xia, R.; Turnbull, G. A.; Andrews, P.; Barnes, W. L.; Samuel, I. D. W.; Bradley, D. D. C. *Adv. Funct. Mater.* **2004**, *14*, 91–97.

conjugated polyelectrolytes,<sup>22,23</sup> like the corresponding poly(phenylenesulfonates),<sup>24,25</sup> tend to form aggregates in water. It has been shown that it is possible to break these aggregates using an organic cosolvent,<sup>22</sup> and with the fluorene copolymer polyelectrolyte poly{1,4-phenylene[9,9-bis(4-phenoxybutyl)sulfonate)]fluorene-2,7-diyl} copolymer (PBS–PFP) in aqueous solution we have shown by both NMR spectroscopy and small angle neutron scattering (SANS) that the nonionic surfactant *n*-dodecyl pentaerythritol ether (C<sub>12</sub>E<sub>5</sub>)<sup>8,10,23</sup> can also induce breakup of aggregates, leading to marked enhancement and a blue shift in the polymer fluorescence. For biological applications it would be desirable to have a biocompatible surfactant to achieve this. In contrast, single-chain cationic surfactants, such as cetyltrimethylammonium bromide (CTAB),<sup>9</sup> neutralize the PBS–PFP charge, but do not break up the aggregates. Thus, a complicated interplay between electrostatic and hydrophobic interactions is involved in the complicated phase behavior in these systems.

Our target for biosensor applications is to obtain a biocompatible surfactant which will break up the conjugated polyelectrolyte aggregates. Lecithin would seem to be the obvious choice, but natural lecithins suffer the complication of being mixtures with varying degrees of purity, and while highly pure synthetic phospholipids avoid this complication, their phase behavior is frequently far from clear. Considerable effort has recently been devoted to the development of new, efficient surfactants that are biodegradable and biocompatible. Amino acid-based derivatives constitute a new class of such biocompatible surfactants with excellent surface properties, quick biodegradation, and low toxicity. All these features make them an outstanding clean and safe alternative to conventional surfactants and very good systems for our applications.<sup>26</sup> An excellent example is 1,2-dilauryl-3-acetylglycyl-*rac*-glycerol (1212R), which can act as a synthetic alternative to lecithin.<sup>27–28</sup> In addition to its good surfactant properties, it is also available in a reasonable state of purity, such that it is possible to obtain a detailed understanding of its phase behavior and interaction with other molecules.

In this work, we combine the valuable spectroscopic and photophysical properties of PBS–PFP and the good surface properties of 1212R to produce a stable, water-soluble aggregate in which the polymer is present as isolated chains, which is likely to make this aggregate valuable for sensing applications of biological systems. The nature of this aggregate has been studied by a combination of spectroscopic and photophysical measurements coupled with preliminary SANS experiments.

## Experimental Section

**Materials.** PBS–PFP (Figure 1) was synthesized by condensation of 2,7-dibromo-9,9-bis(4-sulfonylbutoxyphenyl)fluorene and 1,4-phenylenediboric acid using Pd(PPh<sub>3</sub>)<sub>4</sub> as catalyst.<sup>8</sup> A solution of PBS–PFP with a concentration  $9.6 \times 10^{-3}$  g/L (corresponding to

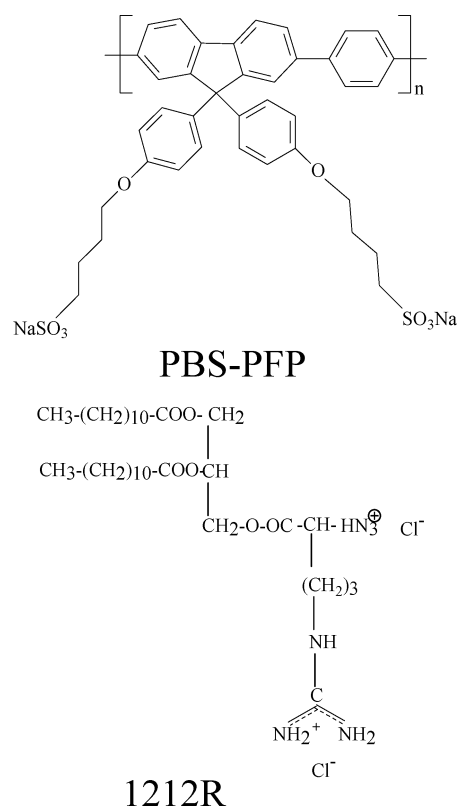


**Figure 1.** Structure of PBS–PFP and 1212R.

about  $1.3 \times 10^{-5}$  (mol of monomer)/L) was freshly prepared and was stirred overnight before use.

The amino acid glyceride conjugate 1-*O*-(L-arginyl)-2,3-*O*-dilauroyl-*sn*-glycerol dichlorohydrate (1212R)<sup>29</sup> was prepared through synthetic chemical routes, as described previously.<sup>30–32</sup> Its structure is also shown in Figure 1. This contrasts with some of the other amino acid-based surfactants<sup>33</sup> which have been produced through enzymatic methods.

For the photophysical experiments, freshly prepared aqueous stock solutions of surfactant were used, with a concentration around  $10^{-3}$  M. From this, more dilute solutions were obtained for experiments over the whole surfactant concentration range used in this study ( $3 \times 10^{-8}$  to around  $10^{-3}$  M). Milli-Q Millipore water was used to prepare the solutions. For SANS measurements, samples were prepared in D<sub>2</sub>O (Goss Scientific Instruments, 99.9% D minimum). For SANS, the polymer and surfactant concentrations of the system studied were 0.42 mg/mL and  $1 \times 10^{-3}$  M, respectively.

**Instrumentation and Methods.** Absorption and luminescence spectra were recorded on Shimadzu UV-2100 and Jobin-Ivon SPEX Fluorolog 3-22 spectrometers, respectively. Fluorescence spectra were registered with excitation at 381 nm and were corrected for the wavelength response of the system. All samples were kept in the absence of light. Fluorescence quantum yields were measured using quinine sulfate in 0.5 M sulfuric acid as the standard.<sup>34</sup>

Fluorescence decays were measured using a home-built time-correlated single-photon-counting apparatus consisting of an IBH NanoLED ( $\lambda_{\text{exc}} = 373$  nm) as the excitation source, a Jobin-Ivon monochromator, a Philips XP2020Q photomultiplier, and a Canberra

(21) Knaapila, M.; Stepanyan, R.; Lyons, B. P.; Torkkeli, M.; Monkman, A. P. *Adv. Funct. Mater.* **2006**, *16*, 599–609.

(22) Wang, S.; Bazan, G. C. *Chem. Commun.* **2004**, 2508–2509.

(23) Knaapila, M.; Almásy, L.; Garamus, V. M.; Pearson, C.; Pradhan, S.; Petty, M. C.; Scherf, U.; Burrows, H. D.; Monkman, A. P. *J. Phys. Chem. B* **2006**, *110*, 10248–10257.

(24) Rulkens, R.; Wegner, G.; Thurn-Albrecht, T. *Langmuir* **1999**, *15*, 4022–4025.

(25) Bockstaller, M.; Köhler, W.; Wegner, G.; Vlassopoulos, D.; Fytas, G. *Macromolecules* **2001**, *34*, 6359–6366.

(26) Morán, M. C.; Pinazo, A.; Pérez, L.; Clapés, P.; Angelet, M.; García, M. T.; Vinardell, M. P.; Infante, M. R. *Green Chem.* **2004**, *6*, 233–240.

(27) Pérez, L.; Infante, M. R.; Pons, R.; Morán, C.; Vinardell, P.; Mitjans, M.; Pinazo, A. *Colloids Surf., B* **2004**, *35*, 235–242.

(28) Pérez, N.; Pérez, L.; Infante, M. R.; García, M. T. *Green Chem.* **2005**, *7*, 540–546.

(29) Pérez, L.; Infante, M. R.; Angelet, M.; Clapes, P.; Pinazo, A. *Prog. Colloid Polym. Sci.* **2004**, *123*, 210–216.

(30) Pérez, L.; Torres, J. L.; Manresa, A.; Solans, C.; Infante, M. R. *Langmuir* **1996**, *12*, 5296–5301.

(31) Pérez, L.; Pinazo, A.; Rosen, M. J.; Infante, M. R. *Langmuir* **1998**, *14*, 2307–2315.

(32) Pinazo, A.; Wen, X.; Pérez, L.; Infante, M. R.; Franses, E. I. *Langmuir* **1999**, *15*, 3134–3142.

(33) Infante, M. R.; Pérez, L.; Pinazo, A.; Clapés, P.; Morán, M. C.; Angelet, M.; García, M. T.; Vinardell, M. P. *C. R. Chim.* **2004**, *7*, 583–592.

(34) *Standards in Fluorescence Spectrometry*; Miller, J. N., Ed.; Chapman and Hall: London, 1981.

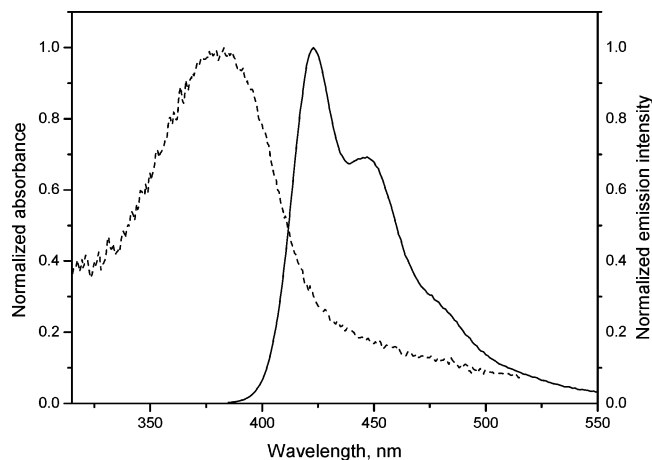


**Figure 2.** Normalized absorption and emission spectra of PBS-PFP in aqueous solutions,  $\lambda_{\text{exc}} = 381$  nm.

Instruments time-to-amplitude converter and multichannel analyzer. Alternate measurements (1000 counts per cycle), controlled by Decay software (Biodinâmica, Portugal), of the pulse profile at 337 or 356 nm and the sample emission were performed until  $(1-2) \times 10^4$  counts at the maximum were reached. The fluorescence decays were analyzed using the modulating functions method of Striker with automatic correction for the photomultiplier “wavelength shift”.<sup>35</sup>

SANS measurements were carried out at the LOQ beamline at the ISIS Facility, Rutherford Appleton Laboratory (U.K.).<sup>36</sup> The LOQ instrument at ISIS uses incident wavelengths between 2.2 and 10 Å sorted by time-of-flight with a sample to detector distance of 4.1 m, resulting in a  $Q$  range between 0.006 and  $0.24 \text{ Å}^{-1}$ . The samples in quartz cuvettes (Hellma) of 2 mm path length were placed in a thermostat and kept at  $25.0 \pm 0.5$  °C during the measurements. The raw data were corrected for the transmission,  $\text{D}_2\text{O}$  background, sample cell, and detector efficiency. The 2D scattering patterns were azimuthally averaged and converted to an absolute scale. The data for one sample were collected for 1 h on average.

## Results and Discussion

The conjugated polyelectrolyte PBS-PFP forms a dispersion in water<sup>10</sup> which shows a broad absorption around 381 nm and a structured fluorescence ( $\lambda_{\text{max}} = 424, 448, \text{ and } 475$  nm (shoulder)), Figure 2. Upon adding different concentrations of the cationic arginine-based surfactant 1212R, the shapes of both the absorption and emission spectra are not significantly affected, but the spectra are blue shifted, and their intensities increase. This is similar to what is seen with the breakup of aggregates of this polymer upon adding  $\text{C}_{12}\text{E}_5$ <sup>8</sup> and in contrast to what has been observed when PBS-PFP interacts with several tetraalkylammonium cationic surfactants with different structures (alkyl chain length, counterion, single or double alkyl chain).<sup>9</sup> The interaction with these cationic surfactants leads to the appearance of a new emission band ( $\sim 525$  nm) which may be due to the increase of PBS-PFP aggregation favored by charge neutralization of the anionic polyelectrolyte and by hydrophobic interactions involving the surfactant alkyl chains, leading to energy hopping to defect sites. In contrast, the same green band is not observed by adding either tetramethylammonium hydroxide or tetramethylammonium chloride, where hydrophobic interactions are likely to be minimal.

The major changes in the absorption spectra upon addition of 1212R are shown in Figure 3, where a blue shift of more than

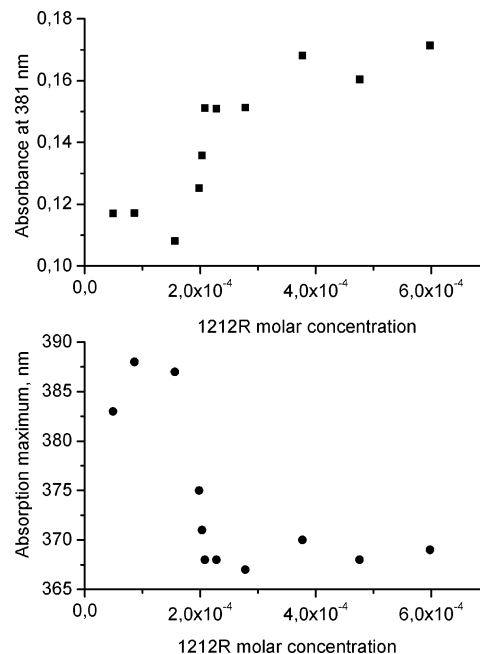


**Figure 3.** Maximum absorbance and absorption wavelength as functions of the 1212R molar concentration.

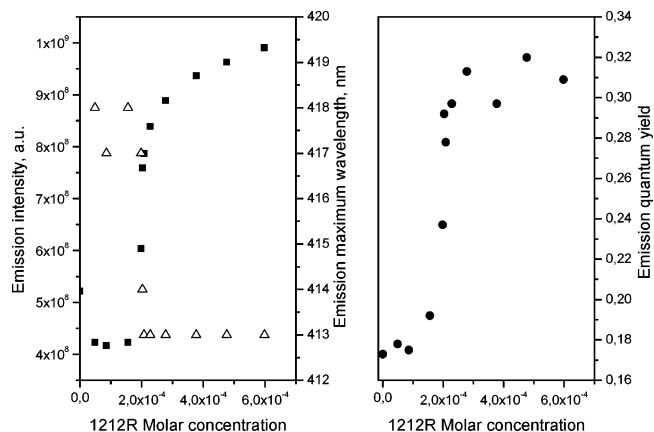


**Figure 4.** Fluorescence intensity (squares), maximum emission wavelength (triangles), and emission quantum yield (circles) as functions of the 1212R molar concentration.

10 nm and an increase in absorbance of about 50% is seen on adding surfactant. These changes do not happen progressively, but instead show a sharp change for 1212R concentrations around  $2 \times 10^{-4}$  M.

The same kind of behavior is observed in the emission spectra, as shown in Figure 4. Again, a break point is seen at a surfactant concentration of about  $2 \times 10^{-4}$  M. At this concentration, the polymer emission intensity and the fluorescence quantum yield are doubled and the emission maximum is blue-shifted by around 10 nm.

Although this is at the limit of the time resolution of our system, qualitatively it seems that the polymer lifetime is longer in the presence of 1212R ( $\tau = 0.48$  ns,  $5.98 \times 10^{-4}$  M) than with the free polymer (0.26 ns).<sup>8</sup> Similar effects were observed following the interaction of PBS-PFP with the nonionic surfactant  $\text{C}_{12}\text{E}_5$ .<sup>8</sup> Although these effects could be explained either by changes in the environment resulting from surfactant complexation<sup>37</sup> or by surfactant-induced breakup of polymer aggregates,<sup>6</sup> the former explanation does not seem to be the

(35) Striker, G.; Subramaniam, V.; Seidel, C. A. M.; Volkmer, A. *J. Phys. Chem. B* **1999**, *103*, 8612–8617.

(36) Heenan, R. K.; Penfold, J.; King, S. M. *J. Appl. Crystallogr.* **1997**, *30*, 1140–1147.

(37) Chen, L.; Xu, S.; McBranch, D.; Whitten, D. *J. Am. Chem. Soc.* **2000**, *122*, 9302–9303.



dominant effect, since the lowest energy absorption band of fluorene is relatively insensitive to solvent polarity,<sup>38</sup> whereas breaking up of polymer aggregates by incorporating PBS–PFP/surfactant aggregates explains both the blue shift and the increased quantum yield.<sup>8</sup>

In water, C<sub>12</sub>E<sub>5</sub> forms elongated cylindrical micelles which grow with concentration, temperature, or solute incorporation,<sup>39</sup> and support in that case for incorporation of PBS–PFP into such micelles comes from <sup>1</sup>H NMR spectra and from the dramatic increases in the fluorescence quantum yield, indicating polymer dissolution.<sup>8</sup> This has recently been confirmed by SANS measurements.<sup>23</sup> It seems probable that the observed changes in the spectroscopic properties of PBS–PFP when interacting with 1212R can also be due to polymer dissolution upon incorporation in micellar-type aggregates with 1212R.

As far as we know, no papers have been published on the aggregation behavior of this recently synthesized surfactant, 1212R. However, studies carried out on a structurally related diacylglycerol amino acid-based surfactant having two fatty chains with 10 carbon atoms instead of the 12 carbon atom chains, 1-*O*-(L-arginyl)-2,3-*O*-didecanoyl-*sn*-glycerol dichlorohydrate (1010R),<sup>40</sup> demonstrate that this surfactant shows unconventional aggregation behavior, with two “critical micelle concentrations” (cmc’s) inferred from different techniques:  $4 \times 10^{-5}$  M detected by surface tension and  $5 \times 10^{-4}$  M detected by conductivity and fluorescence.<sup>29</sup>

Moreover, recent static light scattering studies with extremely dilute solutions of 1010R<sup>40</sup> show that, at concentrations as low as  $5 \times 10^{-6}$  M, the scattered intensity was significant. From the angular dependence and molecular weight of the aggregates a vesicular structure is suggested. Increasing the surfactant concentration induces a vesicle-to-ribbon transition at concentrations of about  $5 \times 10^{-4}$  M. This transition is accompanied by a strong decrease in scattered intensity and change in the angular dependence of scattering. Decreasing the pH at a fixed concentration can also induce the same transition. This phase behavior explains the observation that two widely different critical micelle concentrations are determined using different techniques.

A similar behavior can be expected in the case of 1212R. It is reasonable that, due to the longer alkyl chains, these cmc values will probably be lower.

These two cmc values also seem to have an important role in our photophysical study. At low surfactant concentrations, a sharp increase in the solution scattering at 381 nm is seen with mixtures of the conjugated polyelectrolyte and surfactant for 1212R molar concentrations up to around that of the polymer repeat units ( $< 2 \times 10^{-5}$  M), while for higher surfactant concentrations, the scattering remains relatively constant. This increase in light scattering is probably due to formation of the first type of aggregates (probably vesicles) formed upon neutralization of the polymer charge.

On increasing the surfactant concentration, a break point is observed in our photophysical study in the absorption and emission spectral properties at concentrations around  $2 \times 10^{-4}$  M (Figures 3 and 4), very close to the second cmc observed for 1010R. We suggest that, as with that system, this can also be attributed to a vesicle-to-ribbon transition. This kind of vesicle-to-ribbon transition appears to be characteristic of arginine

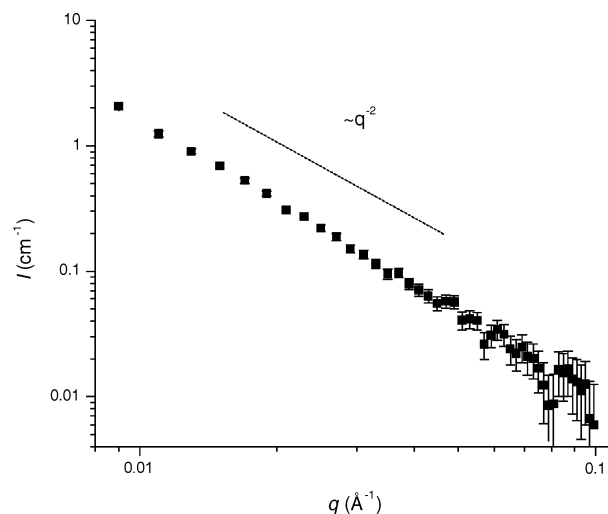


**Figure 5.** SANS data of an aqueous PBS–PFP/1212R mixture measured at 25 °C. The solutions contained 0.42 mg/mL PBS–PFP in a 1 mM 1212R solution. A dashed line shows the slope of the ideal sheetlike particles for comparison.

glyceride conjugate surfactants, such as 1010R and 1212R, and has not been observed for dilute aqueous solutions of the corresponding single-chain and dimeric arginine-based cationic surfactants. Instead, these tend to form spherical micelles in dilute solutions. The only other case we are aware of where such twisted-ribbon structures appear to replace spherical micelles at low concentrations is with gemini surfactants with longer spacer groups.<sup>41</sup> In these cases, no appreciable increase of the PBS–PFP emission quantum yield is observed, as will be discussed elsewhere.

This explanation of the strong blue shift and increase in the fluorescence quantum yield with 1212R resulting from the vesicle-to-ribbon transition implies that long, ribbonlike structures are responsible for the spectroscopic changes. Such structures closely resemble the elongated cylindrical micelles formed by C<sub>12</sub>E<sub>5</sub>, which can also be thought to disrupt the polymer aggregates and to produce isolated PBS–PFP monomers incorporated inside them. It seems reasonable that both the breakup of conjugated polymer aggregates and their incorporation as single chains in water-free environments, such as those present in large surfactant aggregate structures, are key factors in inducing an increase in the PBS–PFP fluorescence quantum yield.

The above results indicate that interaction of the conjugated polyelectrolyte with 1212R aggregation seems to have an important role in improving the photophysical properties of PBS–PFP in aqueous solution (increase of the emission quantum yield). SANS experiments were carried out with the pure surfactant at several concentrations and at a constant 1212R concentration of  $5 \times 10^{-3}$  M with PBS–PFP at several concentrations to gain insight into the aggregation behavior of aqueous 1212R and PBS–PFP/1212R systems. Unfortunately, the concentration ranges readily accessible for photophysical and SANS measurements are not the same, and SANS measurements at the very low concentrations employed in our photophysical investigations are impractical. Hence, we made a preliminary measurement with an order of magnitude more concentrated sample. However, despite the differences in the concentration region studied, we feel that a tentative idea is obtained from these measurements.

Figure 5 plots the SANS data of the PBS–PFP/1212R mixture when 0.42 mg of polymer has been added to 1 mL of 1 mM

(38) Suzuki, H. *Bull. Chem. Soc. Jpn.* **1959**, 32, 1357–1361.

(39) (a) Nilsson, P. G.; Wennerström, H.; Lindman, B. *J. Phys. Chem.* **1983**, 87, 1377–1385. (b) Kato, T.; Anzai, S. I.; Takano, S.; Seimiya, T. *J. Chem. Soc., Faraday Trans. 1* **1989**, 85, 2499–2506. (c) Menge, U.; Lang, P.; Findenegg, G. H.; Strunz, P. *J. Phys. Chem. B* **2003**, 107, 1316–1320.

(40) Pinazo, A.; Pérez, L.; Infante, M. R.; Pons R. *Phys. Chem. Chem. Phys.* **2004**, 6, 1475–1481.

(41) Weihs, D.; Danino, D.; Pinazo-Gassol, A.; Pérez, L.; Franses, E. I.; Talmon, Y. *Colloids Surf., A* **2005**, 255, 73–78.

1212R solution. A distinctive slope of approximately  $-2$  is seen over the whole observation window examined (6–60 nm). This provides preliminary evidence for the existence of two-dimensional particles, possibly with sheetlike structures, although Gaussian chains cannot be excluded. More detailed SANS experiments are planned to confirm this. As described above, PBS–PFP is not water soluble but can be dissolved in aqueous  $C_{12}E_5$ . If the  $C_{12}E_5$  concentration is not sufficiently high in the aqueous PFS–PFP/ $C_{12}E_5$  mixture, the system appears cloudy and SANS data indicate the presence of large, poorly dissolved particles.<sup>23</sup> As no evidence for such large, poorly dissolved particles is observed here, we suggest that 1212R acts as a cosolvent in water. The putative sheetlike feature might instead correspond to 1212R “ribbons” reported for the ultradilute aqueous analogous surfactant 1010R.<sup>40</sup> Although lipid phases involving ribbons of finite width have been known for a long time,<sup>42</sup> rather less is known about them than many of the other structures commonly observed with amphiphile systems. However, their formation could be in accord with all the photophysical, turbidity, and SANS data.

### Conclusions

As has previously been observed with the surfactant  $C_{12}E_5$ , a marked blue shift (10 nm) of the absorption and emission

maxima together with an increase in the PBS–PFP emission quantum yield is induced by 1212R (concentration around  $2 \times 10^{-4}$  M) when a vesicle-to-ribbon transition is produced. The dissolution of the polymer by becoming enclosed in the 1212R ribbon aggregates is suggested to be responsible for this behavior. SANS experiments support the idea of this dissolution behavior and give evidence for two-dimensional aggregates in an aqueous PBS–PFP/1212R mixture for higher concentrations.

**Acknowledgment.** The SANS experiments have been supported by the European Commission under the 6th Framework Programme through the key action Strengthening the European Research Area, Research Infrastructures, Contract No. HII3-CT-2003-505925. We are indebted to Dr. S. King of the Rutherford Appleton Laboratory for assistance with the SANS measurements and in addition to Dr. J. Seixas de Melo and Mr. J. Pina (Universidade de Coimbra) for the fluorescence lifetime measurements. MEC and FEDER are thanked for financial support through Project MAT2004-03827 and POCI/FCT/FEDER through Project POCI/QUI/58291/2004. We are grateful for further funding for this collaboration through MEC/CRUP (Acções Integradas) and the European Union COST Action D15 WG 0017-00. Universidad de Burgos is also thanked for financial support of a short stay of M.J.T. at the Universidade de Coimbra.

LA0612217

(42) Luzzati, V.; Tardieu, A. *Annu. Rev. Phys. Chem.* **1974**, *25*, 79–94.